STM Reveals Surface Diffusion of Single Double-Decker Phthalocyanine Molecules at the Solution/Solid Interface

Shammi Rana,§ Kristen N. Johnson,§ Kirill Gurdumov, Ursula Mazur, and K.W. Hipps*

Department of Chemistry and Materials Science and Engineering Program, Washington State University, Pullman, Washington 99163-4630, United States

Corresponding Author: hipps@wsu.edu

ABSTRACT

Scanning tunneling microscopy (STM) was used to observe and quantify single molecule diffusion at the solution/solid and at the argon/solid interface. This work investigates the influence of temperature, solvent, and STM tip on isolated molecular surface diffusion through analysis of the molecular trajectories in sequential STM images. The surface diffusion of Y[C₆S-Pc]₂ in phenyloctane was found to be thermally activated with almost no motion observed at 5 °C; whereas, above 30 °C molecular motion and/or adsorption/desorption are so rapid that it becomes difficult to track single molecules. The surface diffusion of molecules also depended on solvent; solvents with greater dipole moments (and presumably greater interaction with Au(111)) reduced diffusivity. While the absence of solvent (i.e. argon/solid interface), increased diffusivity. At room temperature, the influence of the STM tip was quantified by varying the sample bias voltage, with the diffusion coefficient varying between 0.6 x 10⁻¹⁷ and 16 x 10⁻¹⁷ cm²/s. This is the first quantitative study of single molecule (as opposed to vacancy) diffusion at the solution/solid interface. An important implication of this study is that even in the case of very strong adsorbate-substrate interactions, the STM tip can significantly mobilize surface molecules and thereby enhance the formation of self-assembled films. Moreover, because the tip induced displacements are not unidirectional, one cannot diagnose tip induced motion by analyzing the displacements at one set-point and scan rate. Particular care must be taken in any STM based studies of self-assembly kinetics at the solution-solid interface.

KEYWORDS: surface diffusion, tracking, scanning tunneling microscopy, solution/solid interface, diffusion coefficient.

Surface diffusion of adsorbates (adatoms, atomic clusters or molecules) is a key subject in surface-interface science and nanotechnology and has received much interest in the last two decades. Surface diffusion plays a significant role in epitaxial growth of thin-films, self-assembly, heterogeneous catalysis, growth of crystals, surface phase formation, sintering, and other processes. While the diffusion of adsorbates has been studied extensively under ultrahigh vacuum (UHV) conditions using a variety of analytical techniques; such as, field ion microscopy, and scanning probe microscopy, much less is known about the dynamics of adsorbates at the solution/solid interface. At the solution/solid interface adsorbate motion, typically, cannot be captured with molecular resolution within the accessible temperature range of available techniques. Nevertheless, molecular surface diffusion at the solution/solid interface is a topic of fundamental interest. By visualizing the mobility of atoms or adatoms over time, it is feasible to extract valuable mechanistic and kinetic information regarding the manner in which the relevant species diffuse.

Previous studies of on-surface adsorbate diffusion have described the mechanism as thermally activated hopping, where the adsorbate moves between adjacent energetically favorable adsorption sites. ¹¹⁻¹³ Hopping between nearest-neighbor surface sites is categorized as a "short-hop" while movement of multiple lattice spaces is called a "long-hop". The overall diffusion rate is dominated by short-uncorrelated hops for adatoms and at low temperature, while the "long-hop" case contributes more at increased temperature and in cases of weaker adsorbate-substrate interaction. ^{14,15} To date, the majority of surface diffusion studies conducted with STM involved the diffusion of atoms in ultra-high vacuum (UHV) conditions, ^{16,17} or at the electrolyte/solid interface. ¹⁸⁻²⁰ STM studies on diffusion of large organic molecules on surfaces in UHV are also well represented in the literature. ^{10,15,21}

Weckesser et al. investigated the surface diffusion of a 4-trans-2-(pyrid-4-yl-vinyl)benzoic acid (PVBA) on the anisotropic Pd(110) surface at sample temperatures from 27 to 177 °C in UHV.²¹ Molecular motion of hexa-tert-butyldecacyclene (HtBDC) and decacyclene (DC) molecules were investigated with help of STM on the Cu(110) surface where both long (multiple) and single jump motions were observed.¹⁵ Kwon et al. combined STM and density functional theory (DFT) to investigate the one dimensional (1D) motion of 9,10-dithioanthracene (DTA) on the Cu(111) surface. 22 J. V. Barth and coworkers, were the first to study the surface diffusion of molecules from the tetrapyrrole family.²³ They investigated the motion of tetrapyridylporphyrin (TPyP) on the Cu(111) surface with STM at the vacuum/solid interface in the 27-87 °C temperature range and observed 1D surface diffusion. Further, Karina Morgenstern and coworkers have studied the surface diffusion of cobalt phthalocyanine (CoPc) molecules on the Ag(100) surface at low temperature (~50 K) at the vacuum/solid interface.²⁴ They learned that the CoPc molecules rotate and translate on the Ag(100) surface. The surface diffusion of 2Htetraphenylporphyrin (2HTPP) molecule on Cu(111) surface was examined by Bucher et al. with help of STM and X-ray photoelectron spectroscopy (XPS) in UHV, and was found to be nearly $1D.^{25}$

STM has also been used to study the diffusion of molecular vacancies within an organized adlayer in this case intermolecular interactions become highly important and complicate the analysis.^{26,27} Takami and Weiss observed tip and thermally induced sliding (hopping) motion of double-decker phthalocyanine that result in vacancy motion at the solution/HOPG interface.²⁸ We have also reported tip and thermally induced vacancy hopping of double-decker phthalocyanines on both HOPG and on Au(111). ²⁹ We note here that vacancy motion which has been considered in several studies is far different than the motion of isolated molecules because

of the absence of intermolecular interactions. Intermolecular interactions in the self-assembled film in which vacancies are imbedded make it impossible to analyze their motion in terms of molecule-substrate interactions alone. The present study is of molecular diffusion of isolated single molecule adsorbates at the solution/solid interface. We will consider only those molecules far from defects, step edges, and clusters. To the best of our knowledge, there are no reports on surface diffusion of single molecules studied by STM at the solution/solid interface.

Recently, our group has investigated the self-assembly, adsorption, and orientation behavior of a double-decker phthalocyanine Y[C₆S-Pc]₂ complex at the solution/solid interface using STM.²⁹ We discussed the formation of molecular assemblies on different surfaces (Au and HOPG) in terms of molecule–substrate and molecule–molecule interactions and qualitatively discussed the tip-induced diffusion of adlayer vacancies. At lower concentrations (<1 μM), stable isolated single molecules were observed on Au(111) surface. In the present work, we look at how STM can be used to study isolated molecule surface diffusion at the solution/solid interface without the complications of intermolecular interactions associated with vacancy diffusion.

Manipulation and movement of adsorbed atoms and molecules by the STM tip is a field as old as STM itself.³⁰ Numerous studies in UHV under cryogenic conditions have demonstrated that atoms and molecules can be manipulated with an STM tip.³¹ Tip manipulation at the solution-solid interface is also well known.³² For example, one can write structures into porphyrin monolayers by tip manipulation.³³ Vacancies in double-decker phthalocyanine complexes can also be manipulated by the STM tip.²⁹ Sometimes these manipulations are primarily due to direct tip-surface contact,³³ while at other times electric field effects are the principal actors.^{32,34} In the present study we will demonstrate that neither high fields or close contact of the tip are necessary to cause significant increases in the mobility of single molecules

on Au(111). Moreover, we will provide the first quantitative measures of this effect at the solution-solid interface.

The diffusion coefficient of isolated molecules on the Au(111) surface was calculated by tracking them for different lengths of time. The effect on surface diffusion of bias voltage, temperature, and the delay time between two consecutive scans were studied. Molecular surface diffusion on Au(111) was also investigated in the absence of solvent (*i.e.* dry state, under argon). Our results enabled us to gain a better understanding of the complex molecular motion at the solution/solid interface and to appreciate the importance of tip-surface interactions in enhancing surface diffusion and the role of the medium in modulating diffusivity.

THEORETICAL AND EXPERIMENTAL METHODS

Materials. 1-Phenyloctane (1-PO) (>98.0%) purchased from TCI America, 1-octanol (99%) purchased from Acros Organics, and *n*-octane, extra dry (99%+) purchased from Acros Organics were used as solvents for STM experiments without further purification. Mechanically cutting Pt/Ir wire (80:20 Pt/Ir, 0.011 in. diameter) was used to prepare STM tips. Previously described methods were used to prepare epitaxial Au(111) films on mica with well-defined terraces and single atomic steps .^{35,36} The Au films were about approximately 0.1–0.2 μm thick and had a mean single grain diameter of about 0.5 μm. These small crystal grains showed reconstruction line spacing ranging from 6.3 to about 9.0 nm.

Synthesis of Y[C₆S-Pc]₂. Y[C₆S-Pc]₂, 2,3,9,10,16,17,23,24-octakis(hexylthio)-phthalocyaninato complex was synthesized as described previously. ^{29,37}

STM experiment. By dissolving the Y[C₆S-Pc]₂ complex in each solvent, a stock solution (10 μm) was prepared. To prepare samples for STM experiments, 10 to 20 μL of 0.2–0.005 μM solution of the Y[C₆S-Pc]₂ complex in 1-PO were deposited on an H₂ flame annealed Au(111)

substrate in a custom-made solution cell fitted with a Kalrez o-ring (McMaster-Carr, Elmhurst IL, USA). STM measurements were taken in constant-current mode using a Molecular Imaging Pico Plus scanning probe microscope outfitted with a 1 µm STM scanner. STM images were further analyzed by using SPIP 6.7.8 software.

Single molecule tracking. Single molecule tracks were determined using Matlab (The Mathworks Inc.) programs based on the automated tracking algorithm from Crocker and Grier³⁸ and adapted by Blair and Dufresne.³⁹ The code for our adaptation is provided in the SI. STM images were linearly drift corrected and bandpass filtered to remove noise. Then the position of the molecule center was determined with sub-pixel precision using a centroid method. Once the position of all molecules was determined in all images in a sequence, the trajectory of each individual molecule was determined using the automated tracking algorithm Matlab routine. Only isolated Y[C₆S-Pc]₂ molecules found in the center of Au(111) terraces were include in the analysis. Molecules adsorbed on step edges or adjacent to other molecules were excluded. The uncertainty margin was determined by applying the same analysis procedure to 3-5 immobile markers in the images.

Diffusion coefficient calculation. Single molecule trajectories have determined from the sequences of STM images. In order to systematically assess the dynamics of the molecules on Au(111) we have used a simple approach to determine mean-squared displacement in the diffusion of Y[C₆S-Pc]₂ molecules, where the time-averaged mean squared displacement (TAMSD) for a single particle was calculated using the following equation:

$$\langle r^2 \rangle = \frac{1}{N-n} \sum_{i=1+n}^{N} (x_i - x_{i-n})^2 + (y_i - y_{i-n})^2, \quad n = 1, ..., N$$
 (1)

where x_i and y_i is the particles position in frame i. Here the trajectory over N total number of images in the sequence has been parameterized by the frame number i and the lag time Δt

between subsequent frames. Giving $N\Delta t$ as the total collection time for the sequence and n the lag time in number of frames. The lowest lag time appears at n = 1 and the largest at n = N. This method is referred to as internal averaging and allows for good estimates of TAMSD at short lag times. Note, the slow scan direction during STM image collection is inverted between subsequent STM images leading to different positions in the image having different collection times. Here, we used the average collection time because the time difference, most notable at the top and bottom of the images, will alternate between shorter and longer than the average time. Additionally, the time difference is not significant for the center of the image where most of the molecules are found. For normal or Brownian diffusion, the mean squared displacement is related to diffusion through the following equation¹¹:

$$\langle r^2 \rangle = 2dDt \tag{2}$$

where d is the dimensionality (in this case 2), D is the diffusion coefficient, and t is the analysis time (or Δt time lag). A plot of $\langle r^2 \rangle$ vs. time is a useful way to categorize different types of diffusion. If the plot is linear then the diffusion can be categorized as normal diffusion. If the plot has a power law relationship:

$$\langle r^2 \rangle = 2dDt^{\alpha} \tag{3}$$

where α is the anomalous exponent, then the diffusion is categorized as anomalous. Anomalous diffusion, is considered sub-diffusive when $\alpha < 1$ and superdiffusive when $\alpha > 1$. These terms have been used to describe a variety of physical scenarios such as protein diffusion within a cell, diffusion in heterogeneous medium, or cellular active transport. A limitation of TAMSD based analysis is that apparent subdiffusive behavior in single particle TAMSD vs. time plots can arises from two main effects 1) displacements in TAMSDs are not independent and 2) inherent measurement error has been shown to bias results toward the subdiffusive regime.

Additionally, the stochastic nature of random motion leads to increasing erratic motion of particles at long time periods creating broad displacement distributions requiring a significant amount of data points in order to achieve reasonable accuracies. One possible solution and the one employed in this work, is to perform an ensemble average over all TAMSDs. This approach averages out the effects of noise, but it does not fully account for the broad long-time distribution. To minimize the long time effects only the first 10% of points in the ensemble averaged TAMSD curves were fit with equation 2 as otherwise notable deviations from the linear increase can be observed even for simulated Brownian diffusion. Another reason long time data do not result in increased accuracy is because of the reduced number of data pairs in the time averaging process. 44,45 The experiments involving Y[C₆S-Pc]₂ showed evidence isotropic. 2D diffusion with no preference for diffusion along any particular lattice direction of the substrate.

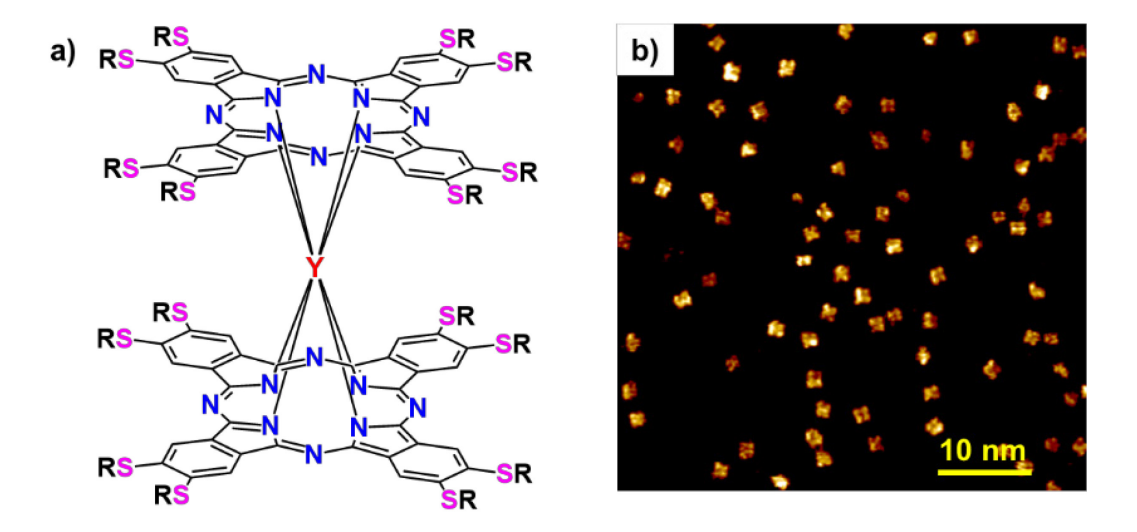


Figure 1. a) Chemical structure of Y[RS-Pc]₂ molecule where R is $-C_6H_{13}$. b) STM image of 0.2 μ M solution of Y[RS-Pc]₂ on Au(111) surface at room temperature. Scanning conditions are V_{bias} (sample) = -0.7 V and I_{tunnel} = 20 pA.

RESULTS AND DISCUSSION

Surface diffusion of Y[C₆S-Pc]₂ at the solution/solid interface

An annealed Au(111) surface was exposed to low concentrations (5-500 nM) of Y[C₆S-Pc]₂ in 1-phenyloctane (1-PO) solution and then studied by STM at room temperature (~22 °C). The Y[C₆S-Pc]₂ molecule is made up of two phthalocyanine rings with eight sulfur-linked side chains that are joined by an yttrium (Y³⁺) metal ion (**Figure 1a**). A size descriptor is problematic for this molecule since the configuration of the alkane chains plays a large role in determining size (see **Figure S0**). Perhaps the best indicator of size on the Au(111) surface is the lattice spacing for the monolayer which is 2.1 nm. The height of the Y[C₆S-Pc]₂ as reported by STM is about 0.5 nm.

At concentrations between 5 and 500 nM, we observed isolated Y[C₆S-Pc]₂ molecules on the Au(111) surface (**Figure 1b**) consisting of four bright lobes. The four lobed structure visible in STM images is attributed to the four benzene rings of the upper phthalocyanine unit. Out of the total 16 sulfur atoms in Y[C₆S-Pc]₂, the eight sulfur atoms on the bottom phthalocyanine unit are directly interacting with Au(111) surface. The stability of the isolated molecules on the surface has been attributed to the strong Au-S interaction. Figure 2a-c show sequential STM scans of a representative surface region where isolated Y[C₆S-Pc]₂ molecules appear to be slowly diffusing over the Au(111) surface. Figure 2e-f displays a zoomed-in portion of consecutive STM images containing two isolated molecules, denoted by green and red X marks. Initially, both molecules are separated by ~3.0 nm, but after three consecutive scans the distance between them has increased to ~4.9 nm. In addition, the molecule indicated by a red X rotates by ~30°. In cases where the four lobed structure of the molecule can be resolved, we observe both translational and rotational motion of the molecules.

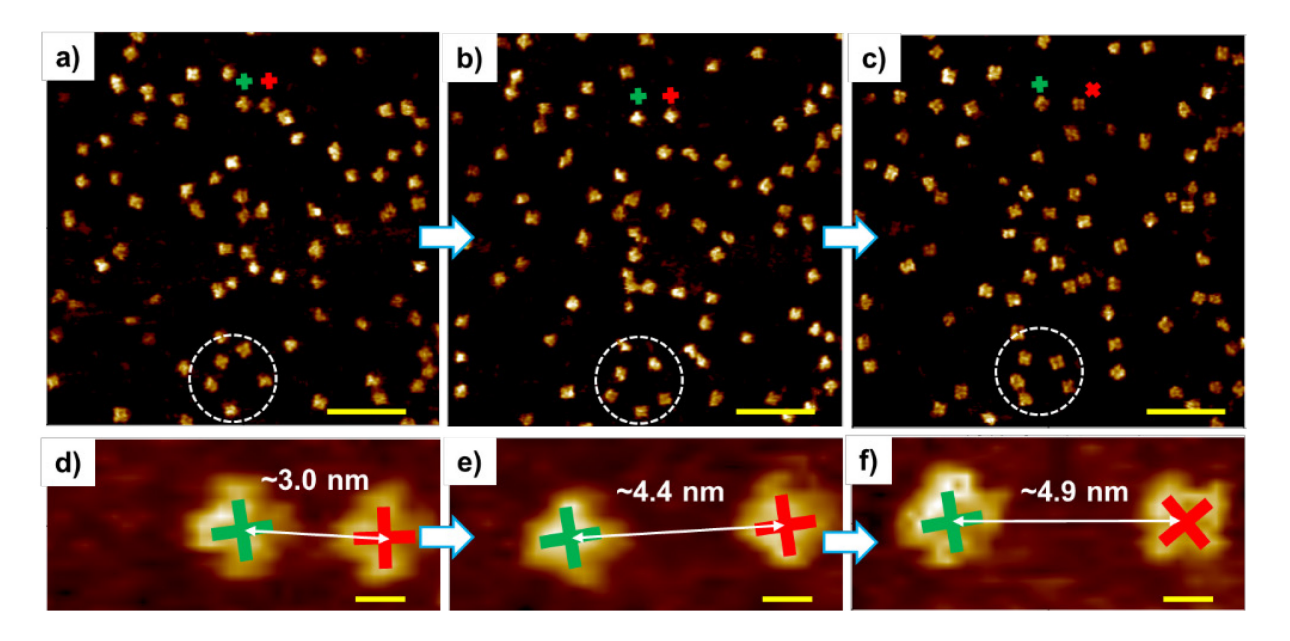


Figure 2. Diffusion of Y[C₆S-Pc]₂ over Au(111) surface. a, b, and c) Sequential STM images showing surface diffusion of Y[C₆S-Pc]₂ at the 1-PO/Au(111) interface. d, e, and f) Zoomed-in portion of above consecutive STM images of selected molecules indicated by green and red X marks, and it clearly shows that the distance between these two molecules increases from ~3.0 nm to ~4.9 nm from the first to third image. Also, the molecule indicated by a red cross undergoes rotational motion as it moves from second to third image. Molecules present in white circled area in three consecutive STM scans clearly display molecular motion. Collection time for each image was 126 s. Once the first scan was completed, the second scan was immediately started. There is no delay time between two images. Scan conditions are $V_{bias} = -0.7 \text{ V}$, $I_{tunnel} = 20 \text{ pA}$. Concentration of Y[C₆S-Pc]₂ is 0.2 μM. Scale bar is 5 nm for a, b, and c images. Scale bar is 1 nm for e, f, and g images.

Rotational-translational motion has been previously reported by Antczak and coworkers for diffusion of a similar system in UHV, cobalt phthalocyanine on Ag(100), where they observed both simple translation and rotational-translational motion.²⁴ The resolution of the images in the remainder of this work is generally insufficient to track the rotation of each molecule; therefore, the remaining discussion will be restricted to translational motion only. Based on the data we acquired, we are unable to access the relative roles of translation, translation/rotation, and sequential translation-rotation in our data set.

To study the diffusion of Y[C₆S-Pc]₂ on the Au(111) surface, we used STM images that were collected sequentially and that allowed us to distinguish the position of each molecule in

each frame. The positions of each individual molecule were correlated with the others in order to produce a molecular trajectory throughout the entire image sequence. Figure 2a-c clearly demonstrates the existence of surface diffusion, but two important questions arise: first, can STM be used to track the molecular motion at the solution/solid interface for extended periods of time? Second, can the diffusion coefficient value be calculated by tracking the positions of isolated Y[C₆S-Pc]₂ molecules at the solution/solid interface? To answer these questions, we performed sequential STM scanning of a fixed area at room temperature for up to ~2.5 hours. Then, we examined the motion of individual molecules as they moved at the interface between a 1-phenyloctane solution and Au(111) and determined the corresponding diffusion coefficient value through the *mean-squared displacements* (MSD) method as described (see methods). STM images were corrected for drift by controlling for the motion of immobile defects and/or surface features, i.e., step edges, and only Y[C₆S-Pc]₂ molecules that were separated from adjacent molecules, defects, and step edges by at least 3-5 nm were included in the analysis. By omitting the motion of molecules near step edges and defects, we consider only the motion on Au(111) terraces. By restricting the analysis to only isolated molecules the influence of interactions between adsorbates can be minimized (see Figure S1, with tracked molecules from movie 1 in the SI –Note that the sequence shown in the movie is different from the short highresolution sequence shown in Figure 2). Figure 3a shows a representative MSD vs. lag time plot ensemble averaged over all particles. The blue dashed curve is the best fit to the first 10% of the data points with equation 2, the red solid curve is the best fit of the entire data series to equation 3 and error bars shown are standard error of the mean. Here lag time is the time separation in numbers of frames multiplied by the time to collect a single image. Use of lag time is known as internal averaging and allows for good estimates of MSD at short lag times but suffers from

increasingly statistically correlated displacements at large lag times which may cause deviations from equation 2, illustrated by the red curve which has α =0.52.⁴⁵ Each data point in **Figure 3a** consists of number of molecules multiplied by the number of total images after subtracting the lag time in number of frames data points. For example, the first data point in **Figure 3a** is 40 molecules x (51 images – 1 frame lag time) = 2000 points. The last point consists of 20 molecules x (51 – 50 frame lag time) = 20 points. To minimize statistical error only the first ten percent of data points were fit. The diffusion coefficient for Y[C₆S-Pc]₂ at the 1-PO/Au(111) interface was calculated to be $(1.1 \pm 0.3) \times 10^{-17}$ cm²/s at +0.7 V sample bias voltage (see **Table S1** and **movie 1** in supporting information). **Figure 3b** shows a representative trajectory of two single molecules throughout 51 consecutive images. There appears to be no preference for the direction of motion. Jumps along both the x and y directions are equally probable. Additional evidence for isotropic motion is provided in **Figure S2**.

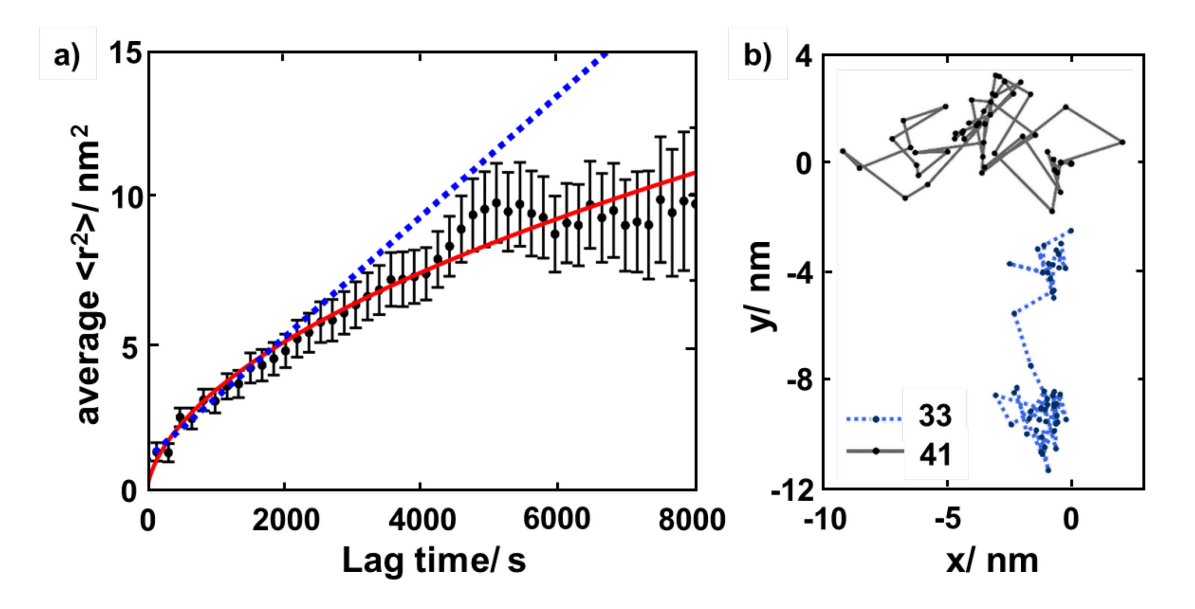


Figure 3. Surface diffusion of Y[C₆S-Pc]₂ molecules and MSD analysis. a) Representative ensemble averaged mean square displacement vs. lag time plot for images collected with bias voltage = ± 0.7 V and tunneling current = 20 pA at room temperature (± 0.2 °C. Error bars are standard error of the mean. The complete sequence consists of 51 images collected at a rate of 169 seconds per image for a total time of 8440 seconds (2hr 20 min). The first 10% (5) points were fitted with equation 2 to give $D = (1.1 \pm 0.3) \times 10^{-17}$ cm²/s (dashed line). The red solid

curve is the entire data series fit with equation 3. b) Position trajectories for two Y[C₆S-Pc]₂ molecules (marked in video of consecutive scans, shown in movie 1) during 51 consecutive scans at room temperature. The mean-square displacement for one frame lag time for molecule 33 is 1.4 nm² and molecule 41 is 3.6 nm².

Diffusion mechanism and temperature dependence

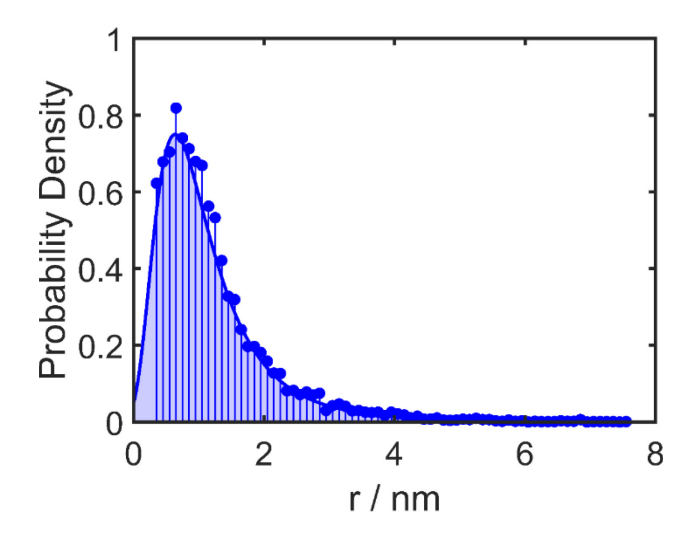


Figure 4. Histogram of displacements fit to gamma distribution function, mean displacement is 1.2 nm. Data from 9,343 jumps with tunneling conditions: +0.7 V and 20 pA.

Typically, one of two mechanisms can explain surface diffusion: the first is hopping of molecules from one surface position to another; and the second is desorption of molecules into solution followed by readsorption on a nearby surface site (flight mechanism). The mechanisms can be distinguished based on the length of the displacements (jumps), short jumps for the hopping mechanism and long jumps for the flight mechanism. **Figure 4** shows the displacement distribution for the molecules at the 1-PO/Au(111) interface, the mean displacement is 1.2 nm for sample bias +0.7 V (The sample at +0.7V relative to the tip). While it is common to relate jump distances to multiples of the surface crystal lattice, in this case the Y[C₆S-Pc]₂ molecules are much bigger than the underlying crystal lattice, the Au(111) lattice constants are 2.88 Å while the diameter of the absorbate is ~20 Å or about seven Au(111) lattice spacings. The present experimental data has an image to image precision of ±0.3 nm and does not have

sufficient resolution to distinguish single Au(111) lattice jump events reliably. The relatively short mean displacement points to the hopping mechanism as the dominant diffusion mechanism for this system. We also observed a molecule during a short jump (**Figure S3**) which is unlikely to be due to desorption/readsorption but might be due to tip induced motion.

It is useful to compare the observed displacementsj of 1 Y[C₆S-Pc]₂ vacancies within the self-assembled monolayer at the 1-PO/Au(111) interface. The distance between adjacent molecules and the observed displacement size, in the self-assembled array is 2.1 nm, but these adsorption sites are heavily influenced by intermolecular interactions and do not seem to be fundamental to the molecule-substrate interaction since we do not see a large contribution of displacements with 2.1 nm distance in the displacement distribution plots, **Figure 4**. This is yet another indicator of the fundamental difference between defect motion as observed previously, and single molecule motion as seen here.

Table 1. Temperature dependency of diffusion coefficient, D, for Y[C₆S-Pc]₂ at the 1-PO/Au(111) interface. Bias conditions are +0.7 V and 20 pA.

Temperature / °C	$D(x 10^{-17}) / cm^2/s$	Number of observations (N)
22	1.1 ± 0.3	13,750
5	0.2 ± 0.3	2,232

Generally, the motion of adsorbates by hopping to nearby preferred absorption sites is considered thermally activated and can be described as Arrhenius type behavior. We used STM measurements and calculated the diffusion coefficient value at two different temperatures at the 1-PO/solid interface to see how temperature affects the diffusion of Y[C₆S-Pc]₂ molecules on the Au(111) surface. At 5 °C, sequential STM scanning shows negligible molecular diffusion, with the majority of the molecules barely moving from their respective position on the Au(111)

surface (see movie 3, **Figure S4**, and **Table S1** in supporting information). Most importantly, at lower temperature, the diffusion coefficient value decreases by an order of magnitude as compared to the value at room temperature, as seen in Table 1. In Table 1 the number of observations (N) is the number of molecules x number of images in the series. Whereas at higher temperature (~30 °C), molecules move so much that it becomes difficult to track a single molecule in consecutive STM scans (**Figure S5**). Attempts to measure diffusion rates above room temperature were frustrated because the temperature of the sample also influences the adsorption/desorption rate. Measurements made at 30 °C (**Figure S5**) show a significant number of molecules appearing and disappearing from the scan area in each image. These changes may be due to enhanced desorption and adsorption rates or the increased molecular motion such that molecules leave and enter the image area.

The diffusion coefficient determined for Y[C₆S-Pc]₂ is much lower than that for a single cobalt phthalocyanine (CoPc) on Ag(100) (calculated to be 2.5 x 10⁻⁴ cm²/s at 27 °C). CoPc/Ag is not Y[C₆S-Pc]₂/Au, but it is the only remotely similar system with available data.²⁴ We attribute the difference in diffusivity to a variety of factors. The first is the presence of a solvent. At the solution-solid interface all available surface sites are consistently occupied by either adsorbate or solvent molecules. In order for an adsorbate to diffuse the solvent occupying the final position must be removed from that site, either through diffusion or desorption. The solvent-substrate interaction strength is therefore a significant factor in determining the diffusion rate of the DD. At the vacuum-solid interface no medium is present to obstruct the diffusive motion of the molecules. As a result, one might conclude that diffusion rates on clean surfaces are greater than diffusion rates on wet surfaces. We observe that the solvent-substrate interaction is extremely important. By choosing a range of solvents that have various degrees of interaction

with the Au(111) surface we were able to modulate the diffusivity of the Y[C₆S-Pc]₂. Using 1-octanol as a solvent no diffusion was observed over a 20-minute time span of continuous image collection, see **Figure S6**. Meanwhile, when the solvent is octane the diffusion coefficient was measured to be 2.4 ± 0.3 (x 10^{-17}) / cm²/s, **movie 4**, similar to the 1-PO case. Finally, in order to test the limiting case of no solvent, we prepared and measured a sample under argon, **Figure S7**. This was achieved by drop casting Y[C₆S-Pc]₂ from toluene and then drying the surface and collecting images in an argon atmosphere to prevent the formation of a surface water layer. In the absence of solvent in an inert atmosphere, we observed increased diffusion such that the Y[C₆S-Pc]₂ molecules were too fast to track by our method.

The oxygen of alkane alcohols is known to donate charge to a metal (Cu, Pt) surface and to have about an order of magnitude greater adsorption energy than a -CH₃ group. ⁴⁶ We expect the same mechanism is active on the Au(111) surface and it is this enhanced adsorption energy that plays the most significant role in slowing the diffusion of Y[C₆S-Pc]₂ on Au relative to octane (and to phenyloctane). Interestingly, we see no significant diffusion for the double decker on Au in air. Presumably, the same mechanism is active since a Au surface in greater than 15% relative humidity is known to be covered with one to two layers of water.

Table 2. Solvent dependency of diffusion coefficient, D, for $Y[C_6S-Pc]_2$ on Au(111) substrate. Bias conditions are +0.7 V and 20 pA.

Solvent	$D (x 10^{-17}) / cm^2/s$	N
1-octanol ^a	≤ 0.2	2,840
1-PO ^b	1.1 ± 0.3	13,750
n-octane ^b	2.4 ± 0.3	3,238
no solvent (argon) ^a	≥ 20	1,540

^a diffusion too slow to observe by current method; ^b diffusion within measurement range.

A second factor in the very slow diffusion of Y[C₆S-Pc]₂ compared to CoPc is the additional Au-S interactions. The Au-S interactions are significant and thought to be the reason that Y[C₆S-Pc]₂ can be found as isolated molecules at all. Y[C₆S-Pc]₂ was also investigated on highly ordered pyrolytic graphite (HOPG), but no isolated molecules were observed.²⁹ Third, the viscosity of the solvent may play a role, since the parts of the solvent molecules not in direct contact with the surface will have Van der Waals barriers to relative motion between solvent molecules. This last possibility is expected to be a weak effect since the viscosities of 1-octanol, 1-phenyloctane, and octane are 7.3 mPa/s, 3.4 mPa/s, and 0.51 mPa/s. These do not easily relate to the observed diffusivity. In cases where the solvents contain the same functionality (e.g.; decane, dodecane, hexadecane) their viscosities in solution may play a greater role. The substrate-molecule interaction and solvent-surface interactions are the major factors determining significantly lower diffusivity of Y[C₆S-Pc]₂ on Au(111) compared to CoPc on Ag(100).

Morgenstern et al's. work with CoPc on Ag(100) demonstrated that the STM tip had no effect on molecular diffusion.²⁴ This was shown by adding a delay time in between consecutive image collection in order to reduce the amount of potential interaction time between the tip and adsorbed molecules. In a similar experiment in the presence of solvent, we observed that the tip does influence the motion of $Y[C_6S-Pc]_2$ on Au(111).

Influence of scanning tip on surface diffusion

While the surface diffusion of Y[C₆S-Pc]₂ is largely dependent on the sample temperature it is also important to consider the contribution of the STM tip. STM imaging necessarily involves interactions between the scanning tip and the sample molecules being observed on the solid surface. The presence of high current density and electric field underneath the scanning tip raises the question of the influence of STM tip on surface diffusion. As detailed in the introduction,

there are numerous studies that demonstrate that the STM tip can be used to move molecules on surfaces. The interactions of a scanning tip with both surface and solvent molecules, and the thermal motion of surface molecules are two important factors that are responsible for inducing molecular displacement on surfaces.²⁴ In order to determine the importance of the scanning tip on the surface diffusion of Y[C₆S-Pc]₂ at the 1-PO/Au(111) interface, we have devised two sets of experiments: 1) dependence of the diffusion coefficient on delay time between images; 2) dependence of the diffusion coefficient on sample bias voltage.

Table 3. Wait time dependence on diffusion coefficient, D, of Y[C₆S-Pc]₂ on Au(111) at +0.7 V, 20 pA, and 22 °C.

Wait time / min	$D (x 10^{-17}) / cm^2/s$	N
0	1.1 ± 0.3	13,750
10	0.3 ± 0.3	1,662

In a first set of experiments, the wait interval between two consecutive STM scans was varied from zero to thirty minutes. In zero waiting interval, the STM tip scans image after image without any delay time. During long waiting intervals, after collecting a single image, the STM tip was stopped and kept stationary within tunneling distance of the sample surface. After waiting a delay time of 10 and 30 minutes, the tip again starts scanning and an additional image is collected. The process is repeated until a set total elapsed time is reached. Au(111) step edges and other surface features were aligned to correct for thermal drift during the wait time (for example images see **Figure S8**). The extended wait time drastically reduces the amount of time the scanning tip spends interacting with each molecule. In images without delay time, a given point on the surface was scanned every 169 seconds while for the 10- and 30-minutes delay time the image collection time was 169 seconds, but the tip crossed a particular point once every 770 or 1900 seconds respectively. The diffusion coefficient value decreased by an order of magnitude

when the scan delay was increased from 0 to 10 minutes, indicating a strong scanning tip dependence on the surface diffusion. In fact, the observed value after 10 minutes is long enough that it is within the error limits of our measurement. This suggests that a 10-minute delay is long enough to significantly reduce the influence of the tip. Data collected at 30 minutes is complicated by adsorption and desorption events and we did not feel confident in assigning a diffusion coefficient. **Table 3** shows the value of the diffusion coefficient calculated at each delay time. If the scanning motion of the STM tip did not contribute to the diffusion of the Y[C₆-S-Pc]₂ molecule at 1-PO/Au(111) surface we would expect to see the same value of diffusion coefficient irrespective of delay time.

Table 4. Sample bias voltage dependent diffusion coefficient for Y[C₆S-Pc]₂ on Au(111) surface at 22 °C and a constant tunneling current of 20 pA.

Bias / V	$D(x 10^{-17}) / cm^2/s$	N
-0.3	16 ± 0.3	966
0.4	9.0 ± 0.3	2,730
0.5	0.6 ± 0.3	11,760
0.7	1.1 ± 0.3	13,750
1.3	1.8 ± 0.3	2,275

To further explore the tip influence on diffusion, sequential STM scanning was performed at different bias voltages ranging from -0.3 V to +1.3 V at constant tunneling current and room temperature. The results of these experiments are shown in **Figure 5a** and the fitted diffusion coefficients are collected in **Table 4**. Results show a bias dependence on the observed diffusion coefficient values. Based on the uncertainties, the values at 0.7 and 1.3 V bias might be the same, but those between +0.5 V and -0.3 V are clearly well outside the standard deviation in our measurements. As the bias voltage approaches zero, the diffusion coefficient value increases. As the bias voltage rises above 0.5 V the diffusion coefficients also increase but much more slowly.

Interestingly, a large bias dependence on surface diffusion was clearly visible in trajectory clouds showing tracks of isolated molecules at low and high bias voltages (**Figure 5b** and **5c**). The molecular displacements are more pronounced between +0.5 and -0.3 V bias voltage than at 0.7 V. A simple possible explanation of this phenomena is that the amount of induced motion is proportional to the height of the tip above the surface. Assuming a simple trapezoidal tunneling barrier, the tip-sample distance, d, can be related to the bias voltage, V, and current, I, through the following relationship 47 :

$$I \cong cV \ e^{-Ad\sqrt{\Phi - (V/2)}} \tag{4}$$

where c is a constant, Φ is the tunneling barrier, and A is 1.02 (Å/eV)^{1/2} when d is in units of angstroms and Φ in units of eV. The tunneling barrier, Φ , was measured for this system by collecting I(z) curves at various bias voltages and the results are plotted in Figure S8. The aggregate data average to 0.82 ± 0.2 eV, and the plot shows a minimum in barrier height near +0.3 eV bias. In addition, we measured the tip distance moved between the current setpoint of 20 pA and saturation of our preamp at 10 nA at 0.3 volts sample bias. Because the current at contact with the surface is expected to be microamps, this is an underestimate of the actual tipsurface distance. What we found was a tip height of about 0.9 nm and we believe the actual distance from the surface at 0.3 V and 20 pA is more than 1.0 nm. At fixed tunneling current, increasing the bias voltage nonlinearly increases the distance between tip and the surface. At low (nearer to zero) bias voltage, interaction between the tip surface and the molecule increases. However, based on the values found for the barrier height and distance from the surface at 20 pA and 0.3 volt, equation 4 predicts at most a 0.2 nm change in height upon increasing the bias to 1.0 V. Thus, it seems unlikely that there is a big change in direct (contact) tip-surface interaction in the 0.2 to 1 volt bias range. Solvent drag between tip and surface also increases as the tip

moves closer to the surface. These two factors together may result in greater motion of molecules on the surface and a higher corresponding diffusion coefficient value.

The local electric field is also a concern. As one varies bias between 0.2 and 1.0 volts, the electric field increases by about a factor of 5 (the distance denominator varies only from about 8 to 10). However, the induced motion decreases as the electric field increases, indication that the electric field is not the primary motivator of molecular motion in this case. There is an additional factor that must be considered. The phthalocyanines are known to have electronic states near 1 eV of the Fermi level. These electronic states can provide a pathway for resonant tunneling, significantly decreasing the tunneling barrier. At fixed current, when the bias is near such resonances, the distance between tip and surface will increase much more than given by equation 4 with a constant value of the barrier height5. It may be that the dip in D near 0.5 eV and that in Φ near 0.3 eV are due to such an electronic resonance. We attempted to collect I(V) curves to determine if any resonant states exist around 0.5 eV, but due to the presence of solvent the spectra were not sufficiently reproducible to provide a definitive answer.

Alternatively, positive biases may enhance the molecule-surface interaction while negative bias voltages reduce the interaction through changes in the effective surface dipole moment. This could explain why large diffusion at negative bias and much less at positive bias is observed.

It is interesting that we do not observe a preference to diffusion parallel to the fast-scanning direction, in fact, we see no preference for jump direction, **Figure S2**. This may have implications concerning the role of solvent drag. There are examples of orienting adsorbed layers through solvent flow control⁴⁸ (it is likely that solvent drag plays a major role). Thus, one might expect that solvent drag would generally lead to a preferential motion along the scan direction –

not seen here. If this conjecture is correct (and we are not sure it is) than solvent drag is not playing a significant role here.

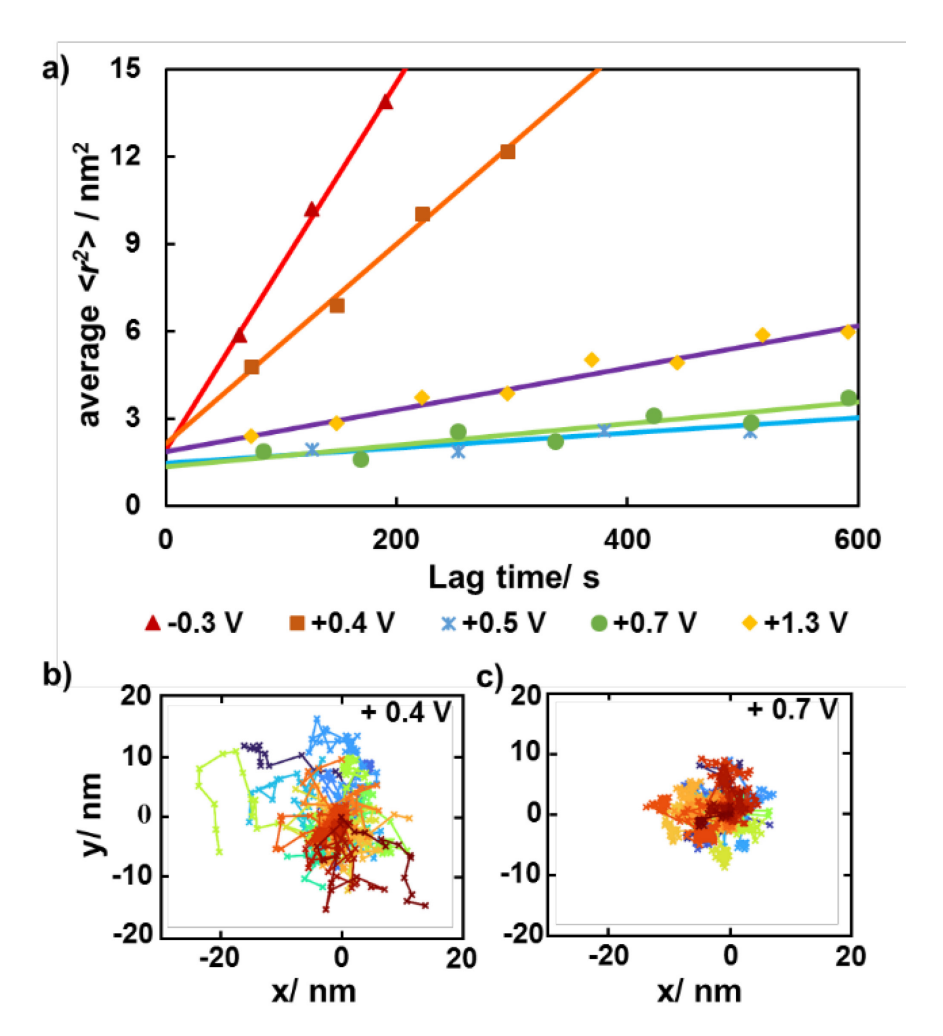


Figure 5. Bias dependence on surface diffusion. (a) Bias voltage dependent of ensemble averaged MSD vs. lag time plots. Each set of data is shown fit the best line (slope/4 is equal to the diffusion coefficient, equation 2). Trajectory clouds showing particle x and y displacements for all particles throughout the entire track for +0.4 V bias (b) and +0.7 V bias (c). Videos of consecutive STM scans at different bias voltage, as shown in supporting information **Table S1** and **movie 2**.

CONCLUSION

STM was used to directly image and track the diffusion of single molecules at the solution/solid and argon/solid interfaces. Based on these measurements, we calculated diffusion coefficient values under various conditions. Consecutive STM scanning enabled us to track a

single molecule for long periods of time, and the diffusion coefficient value was calculated to be between 0.6 and 16 (x 10^{-17}) cm²/s at the 1-PO/solid interface at room temperature while continuously scanning. The surface diffusion of Y[C₆S-Pc]₂ molecules was found to be thermally activated, while also influenced by the STM tip, and the choice of solvent. At low temperatures ($\lesssim 5$ °C), or in 1-octanol solvent, Y[C₆S-Pc]₂ molecules barely move from their respective positions on the Au(111) surface. In fact, the extremely small motion observed might simply be due to positional uncertainty in our experimental data. While at slightly higher temperatures ($\gtrsim 30$ °C), or in the absence of solvent, Y[C₆S-Pc]₂ molecules diffuse so quickly on the STM time scale that they cannot be reliably tracked. We also showed that the tip makes a significant contribution to surface diffusion, with a strong bias dependence (increase in *D* of a factor of 16 between 0.7 and -0.3V) and significantly less motion is observed when the delay time between collected images was increased. Notably, the spatial distribution of the motion does not reflect the scan direction. Thus, diffusion measurements carried out at one set-point and scan rate cannot distinguish tip induced from thermally induced motion.

Unfortunately, it is difficult to separate the tip effects from the native diffusion of the molecule. Our STM also suffers from a relatively slow (on the order of minutes) image collection time. The observation that the diffusion stops at 5 °C is a strong indicator that tip induced motion is not the primary factor in determining the diffusion coefficient. In this work we have determined that the mechanism for surface diffusion of Y[C₆S-Pc]₂ is complex. Rotational and translational motion appears to be at least partially coupled and the diffusion appears to primarily occur through short hops below 30 °C. Adsorption/desorption events become more important at temperatures above 30 °C and interfere with diffusion measurements.

Self-assembled monolayers (SAMs) are clearly formed by a balance of adsorbate-substrate, adsorbate-adsorbate, solvent-substrate, and adsorbate-solvent interactions.^{49,50} The diffusion process is governed by a complex interaction between all four of these, and it plays an important role in determining the kinetics of self-assembly. The observation of tip dependence in diffusion rates of isolated molecules at the solution/solid interface should be carefully considered in any STM study of kinetics of self-assembly. Tip-adsorbate interactions can significantly increase diffusion rates and consequently reduce the time for self-assembly when the intermolecular interactions are strong. On the other hand, if the intermolecular and molecule-substrate interactions are marginal, the tip may destabilize the self-assembled structures. The solvent also has a significant influence on the diffusion rates. Compared with 1-PO, the absence of solvent increases the diffusion rates for isolated Y[C₆S-Pc]₂ molecules on Au(111) surface while the presence of 1-octanol, a solvent with stronger interaction with the substrate, reduces diffusion rates. Diffusion in *n*-octane was similar to that in 1-PO. Compared with the diffusion of other molecules in the porphyrin/phthalocyanine family studied at the vacuum/solid interface, diffusion of Y[C₆S-Pc]₂ molecules on Au(111) surface is much slower. This is likely due to a specific Au-S interaction, but it is also influenced by the medium.

ASSOCIATED CONTENT

Supporting Information. The Supporting Information is available free of charge at XXXXX. Additional details on supporting movies, structure of Y[C₆S-Pc]₂, representative STM images, hopping motion of molecules, tunneling barrier height as a function of bias, and MATLAB code for diffusion analysis (PDF). Example movies (4) of molecular diffusion in consecutive STM images under described conditions (AVI).

AUTHOR INFORMATION

Corresponding Author

K. W. Hipps – Department of Chemistry and Materials Science and Engineering Program,

Washington State University, Pullman, Washington 99163-4630, United States; orcid.org/0000-

0002-5944-5114.

Email: hipps@ wsu.edu

Authors

Shammi Rana - Department of Chemistry and Materials Science and Engineering Program,

Washington State University, Pullman, Washington 99163-4630, United States

Kristen N. Johnson - Department of Chemistry and Materials Science and Engineering

Program, Washington State University, Pullman, Washington 99163-4630, United States;

orcid.org/0000-0003-3622-9686.

Kirill Gurdumov - Department of Chemistry and Materials Science and Engineering Program,

Washington State University, Pullman, Washington 99163-4630, United States

Ursula Mazur - Department of Chemistry and Materials Science and Engineering Program,

Washington State University, Pullman, Washington 99163-4630, United States; orcid.org/0000-

0002-3471-4883

Author Contributions

§ Contributed equally.

Notes

The authors declare no competing financial interest.

26

ACKNOWLEDGMENTS

This works is supported by the US National Science Foundation in the form of grant CHE1807225. We also gratefully acknowledge support from the W. M. Keck Foundation and Washington State University. We thank Professor Jianzhuang Jiang for providing the Y[C₆S-Pc]₂.

REFERENCES

(1) Jamnig, A.; Sangiovanni, D.G.; Abadias, G.; Sarakinos, K. Atomic-Scale Diffusion Rates During Growth of Thin Metal Films on Weakly-Interacting Substrates, *Sci. Rep.*, **2019**, *9*, 6640-6650.

- (2) Woehl, T. J.; Prozorov, T. The Mechanisms for Nanoparticle Surface Diffusion and Chain Self-Assembly Determined from Real-Time Nanoscale Kinetics in Liquid. *J. Phys. Chem. C*, **2015**, *119*, 21261–21269.
- (3) Weber, D.; Sederman, A. J.; Mantle, M. D.; Gladden, L. F. Surface Diffusion in Porous Catalysts. *Phys. Chem. Chem. Phys.* **2010**, *12*, 2619-2624.
- (4) Xia, X.; Xie, S.; Liu, M.; Peng, H. C.; Lu, N.; Wang, J.; Kim, M. J.; Xia, Y. On the Role of Surface Diffusion in Determining the Shape or Morphology of Noble-Metal Nanocrystals. *Proc. Natl. Acad. Sci. U S A.*, **2013**, *110*, 6669-6673.
- (5) Hannon, J. B.; Hibino, H.; Bartelt, N. C.; Swartzentruber, B. S.; Ogino, T.; Kellogg. G. L. Dynamics of the Silicon (111) Surface Phase Transition. *Nature*, **2000**, *405*, 552–554.

- (6) Kingery, W. D. Regelation, Surface Diffusion, and Ice Sintering. *J. Appl. Phys.* **1960**, *31*, 833–838.
- (7) Kellogg, G. L. Field Ion Microscope Studies of Single-Atom Surface Diffusion and Cluster Nucleation on Metal Surfaces. *Surf. Sci. Rep.* **1994**, *21*, 1-88.
- (8) Mo, Y. W.; Kleiner, J.; Webb, M. B.; Lagally, M. G. Activation Energy for Surface Diffusion of Si on Si(001): A Scanning-Tunneling-Microscopy Study. *Phys. Rev. Lett.* **1991**, *66*, 1998-2002.
- (9) Mo, Y. W. Direct Determination of Surface Diffusion by Displacement Distribution Measurement with Scanning Tunneling Microscopy. *Phys. Rev. Lett.* **1993**, *71*, 2923-2926.
- (10) Miwa, J. A.; Weigelt, S.; Gersen, H.; Besenbacher, F.; Rosei, F.; Linderoth, T. R. Azobenzene on Cu(110): adsorption site-dependent diffusion. *J. Amer. Chem. Soc.* **2006**, *128*, 3164-3165
- (11) Gomer, R. Diffusion of Adsorbates on Metal Surfaces. Rep. Prog. Phys., 1990, 53, 917-1000.
- (12) Antczak, G.; Ehrlich, G. Surface Diffusion: Metal, Metals atoms and Clusters; Cambridge University Press: Cambridge, U.K. 2010.
- (13) Somorjai, G. A. Surface Chemistry and Catalysis, Wiley, New York, 1994.
- (14) Dobbs, K. D.; Doren, D. J. Dynamics of Molecular Surface Diffusion: Origins and Consequences of Long Jumps. *J. Chem. Phys.* **1992**, *97*, 3722–3735.

- (15) Schunack, M.; Linderoth, T. R.; Rosei, F.; Lægsgaard, E.; Stensgaard, I.; Besenbacher, F. Long Jumps in the Surface Diffusion of Large Molecules. *Phys. Rev. Lett.* **2002**, *88*, 156102-156105.
- (16) Sändig, N.; Zerbetto, F. Laws of Thermal Diffusion of Individual Molecules on the Gold Surface. *Phys. Chem. Chem. Phys.* **2011**, *13*, 13690–13697.
- (17) Ganz, E.; Theiss, S. K.; Hwang, I. S.; Golovchenko, J. Direct Measurement of Diffusion by Hot Tunneling Microscopy: Activation Energy, Anisotropy, and Long Jumps. *J. Phys. Rev. Lett.* **1992**, *68*, 1567–1570.
- (18) Tansel, T.; Magnussen, O. M. Video STM Studies of Adsorbate Diffusion at Electrochemical Interfaces. *Phys. Rev. Lett.* **2006**, *96*, 026101-026104.
- (19) Yang, Y. C.; Magnussen, O. M. Quantitative Studies of Adsorbate Dynamics at Noble Metal Electrodes by in Situ Video-STM. *Phys. Chem. Chem. Phys.* **2013**, *15*, 12480–12487.
- (20) Guézo, S.; Taranovskyy, A.; Matsushima, H.; Magnussen, O. M. Surface Dynamics of Lead Adsorbates at the Cu(100)–Electrolyte Interface. *J. Phys. Chem. C*, **2011**, *115*, 19336–19342.
- (21) Weckesser, J.; Barth, J. V.; Kern, K. Direct Observation of Surface Diffusion of Large Organic Molecules at Metal Surfaces: PVBA on Pd(110). *J. Chem. Phys.* **1999**, *110*, 5351-5354.
- (22) Kwon, K. Y.; Wong, K. L.; Pawin, G.; Bartels, L.; Stolbov, S.; Rahman, T. S. Unidirectional Adsorbate Motion on a High-Symmetry Surface: "Walking" Molecules Can Stay the Course. *Phys. Rev. Lett.* **2005**, *95*, 166101-166104.

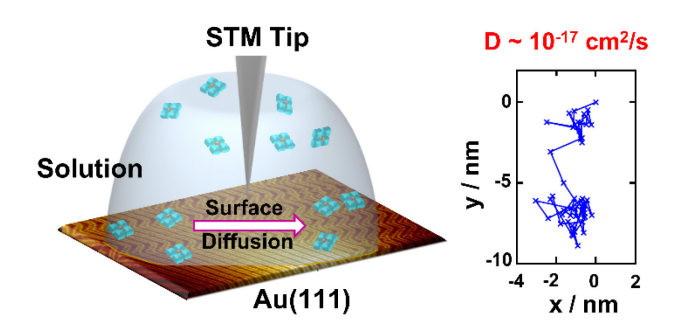
- (23) Eichberger, M.; Marschall, M.; Reichert, J.; Weber-Bargioni, A.; Auwärter, W.; Wang, R. L. C.; Kreuzer, H. J.; Pennec, Y.; Schiffrin, A.; Barth, J. V. Dimerization Boosts One-Dimensional Mobility of Conformationally Adapted Porphyrins on a Hexagonal Surface Atomic Lattice. *Nano Lett.* **2008**, *8*, 4608-4613.
- (24) Antczak, G.; Kaminski, W.; Sabik, A.; Zaum, C.; Morgenstern, K. Complex Surface Diffusion Mechanisms of Cobalt Phthalocyanine Molecules on Ag(100). *J. Am. Chem. Soc.* **2015**, *137*, 14920–14929.
- (25) Buchner, F.; Xiao, J.; Zillner, J.; Chen, M.; Röckert, M.; Ditze, S.; Stark, M.; Steinrück, H. P.; Gottfried, J. M.; Marbach, H. Diffusion, Rotation, and Surface Chemical Bond of Individual 2H-Tetraphenylporphyrin Molecules on Cu(111). *J. Phys. Chem. C*, **2011**, *115*, 24172-24177.
- (26) Urban, C.; Otero, R.; Écija, D.; Trelka, M.; Martín, N.; Gallego, J. M.; Miranda, R. Collective Concerted Motion in a Molecular Adlayer Visualized Through the Surface Diffusion of Isolated Vacancies. *J. Chem. Phys.*, **2016**, *145*, 154706.
- (27) Morgenstern, K.; Lægsgaard, E.; Besenbacher, F. Brownian Motion of 2D Vacancy Islands by Adatom Terrace Diffusion. *Phys. Rev. Lett.*, **2001**, *86*, 5739-5742.
- (28) Takami, T.; Ye, T.; Pathem, D.; Arnold, D.; Sugiura, K.; Bian, Y.; Jing, J.; Weiss, P. Manipulating Double-Decker Molecules at the Liquid-Solid Interface. *J. Am. Chem. Soc.*, **2010**, *132*, 16460-16466.

- (29) Rana, S.; Jiang, J.; Korpany, K. V.; Mazur, U.; Hipps, K. W. STM Investigation of the Y[C₆S-Pc]₂ and Y[C₄O-Pc]₂ Complex at the Solution–Solid Interface: Substrate Effects, Submolecular Resolution, and Vacancies. *J. Phys. Chem. C*, **2021**, *125*, 1421–1431.
- (30) Eigler, D. M.; Schweizer, E. K. Positioning single atoms with a scanning tunnelling microscope. *Nature* **1990**, *344*, 524-526.
- (31) Jacoby, M. 30 years of moving atoms: How scanning probe microscopes revolutionized nanoscience. *C&E News*, https://cen.acs.org/analytical-chemistry/imaging/30-years-moving-atoms-scanning/97/i44 [accessed 1 December 2021].
- (32) Li, M.; den Boer, D.; Iavicoli, P.; Adisoejoso, J.; Uji-I, H.; Van der Auweraer, M.; Amabilino, D. B.; Elemans, J. A. A. W.; De Feyter, S. Tip-Induced Chemical Manipulation of Metal Porphyrins at a Liquid-Solid Interface. *J. Am. Chem. Soc.*, **2014**, *136*, 17418–17421.
- (33) Scudiero, L.; Hipps, K. W. Controlled Manipulation of Self-Organized Ni (II)-Octaethylporphyrin Molecules Deposited from Solution on HOPG with a Scanning Tunneling Microscope. *J. Phys. Chem. C*, **2007**, *111*, 17516-17520.
- (34) Bhattarai, A.; Mazur, U.; Hipps, K. W. Desorption Kinetics and Activation Energy for Cobalt Octaethylporphyrin from Graphite at the Phenyloctane Solution—Graphite Interface: An STM Study. *J. Phys. Chem. C*, **2015**, *119*, 9386-9394.
- (35) Lu, X.; Hipps, K. W. Scanning Tunneling Microscopy of Metal Phthalocyanines: d⁶ and d⁸ Cases. *J. Phys. Chem. B*, **1997**, *101*, 5391–5396.

- (36) Hipps, K. W.; Barlow, D. E.; Mazur, U. Orbital Mediated Tunneling in Vanadyl Phthalocyanine Observed in Both Tunnel Diode and STM Environments. *J. Phys. Chem. B*, **2000**, *104*, 2444–2447.
- (37) Huang, C.; Zhang, Y.; Sun, J.; Bian, Y.; Arnold, D. P. Bis/tris[octakis(hexylthio)phthalocyaninato]Europium(III) Complexes: Structure, Spectroscopic, and Electrochemical Properties. *J. Porphyrins Phthalocyanines*, **2013**, *17*, 673–681.
- (38) Crocker, J. C.; Grier, D. G. J. Methods of Digital Video Microscopy for Colloidal Studies. *Colloid Interface Sci.*, **1996**, *179*, 298–310.
- (39) Blair, D.; Dufresne, E., Georgetown University. The Matlab Particle Tracking Code Repository. http://site.physics.georgetown.edu/matlab/index.html [Accessed 3 June 2021].
- (40) Weiss, M.; Elsner, M.; Kartberg, F.; Nilsson, T. Anomalous Subdiffusion is a Measure for Cytoplasmic Crowding in Living Cells. *Biophys. J.*, **2004**, *87*, 3518–3524.
- (41) Bouchaud, J. P.; Georges, A. Anomalous Diffusion in Disordered Media: Statistical Mechanisms, Models and Physical Applications. *Phys. Reps.*, **1990**, *195*, 131–160.
- (42) Vestergaard, C. L.; Blainey, P. C.; Flyvbjerg, H. Optimal Estimation of Diffusion Coefficients from Single-Particle Trajectories. *Phys. Rev. E.*, **2014**, *89*, 022726-022756.
- (43) Martin, D. S.; Forstner, M. B.; Käs, J. A. Apparent Subdiffusion Inherent to Single Particle Tracking. *Biophys. J.*, **2002**, *83*, 2109–2117.

- (44) Michalet, X. Mean Square Displacement Analysis of Single-Particle Trajectories with Localization Error: Brownian Motion in Isotropic Medium. *Phys. Rev. E.* **2010**, *82*, 041914-041939.
- (45) Kerkhoff, Y.; Block, S. Analysis and Refinement of 2D Single-Particle Tracking Experiments. *Biointerphases* **2020**, *15*, 021201-0212016.
- (46) Sexton, B. A.; Hughes, A. A Comparison of Weak Molecular Adsorption of Organic Molecules on Clean Copper and Platinum Surfaces. *Surf. Sci.*, **1984**, *140*, 227-248.
- (47) Hipps, K. W. Scanning Tunneling Spectroscopy. In *Handbook of Applied Solid State Spectroscopy*, Vij, D. R., Ed.; Springer: Boston, MA, 2006; pp 305-350. DOI:10.1007/0-387-37590-2.
- (48) Lee, S.; Yuan, Z.; Chen, L.; Mali, K.; Mullen, K.; De Feyter, S. Flow-assisted 2D polymorph selection: stabilizing metastable monolayers at the liquid-solid interface. *J. Am. Chem. Soc.*, **2014**, *136*, 7595-7598.
- (49) Yokoyama, T.; Yokoyama, S.; Kamikado, T.; Okuno, Y.; Mashiko, S. Selective Assembly on a Surface of Supramolecular Aggregates with Controlled Size and Shape. *Nature*, **2001**, *413*, 619–621.
- (50) Theobald, J. A.; Oxtoby, N. S.; Phillips, M. A.; Champness, N. R.; Beton, P. H. Controlling Molecular Deposition and Layer Structure with Supramolecular Surface Assemblies. *Nature*, **2003**, *424*, 1029–1031.

TOC Graphic



This study investigates the STM tip and temperature dependence on the surface diffusion of isolated single double-decker phthalocyanine molecules at the solution/solid interface. The results show that the STM tip influences diffusion rates and that is faster in the presence of solvent.